

Suppression of HMGB1 Released in the Glioblastoma Tumor Microenvironment Reduces Tumoral Edema

Bangxing Hong,¹ Kamaldeen Muili,^{2,3} Chelsea Bolyard,^{2,4} Luke Russell,^{2,5} Tae Jin Lee,¹ Yeshavanth Banasavadi-Siddegowda,^{1,6} Ji Young Yoo,¹ Yuanqing Yan,¹ Leomar Y. Ballester,^{1,7} Kurt H. Bockhorst,⁸ and Balveen Kaur^{1,2}

¹Department of Neurosurgery, McGovern Medical School, University of Texas Health Science Center, Houston, TX, USA; ²The James Comprehensive Cancer Center, The Ohio State University, Columbus, OH, USA; ³College of Health and Human Services, Bowling Green State University, Bowling Green, OH, USA; ⁴OhioHealth Research & Innovation Institute, OhioHealth, Columbus, OH, USA; ⁵Vyriad, Rochester, MN, USA; ⁶Surgical Neurology Branch, NINDS, NIH, Bethesda, MD, USA; ⁷Department of Pathology and Laboratory Medicine, McGovern Medical School, University of Texas Health Science Center, Houston, TX, USA; ⁸Department of Diagnostic and Interventional Imaging, University of Texas Health Science Center, Houston, TX, USA

HMGB1 is a ubiquitously expressed intracellular protein that binds DNA and transcription factors and regulates chromosomal structure and function. Under conditions of cell death or stress, it is actively or passively released by cells into the extracellular environment, where it functions as damage-associated molecular pattern (DAMP) that orchestrates pro-inflammatory cytokine release and inflammation. Our results demonstrate that HMGB1 is secreted in the tumor microenvironment after oncolytic HSV (oHSV) infection *in vitro* and *in vivo*. The impact of secreted HMGB1 on tumor growth and response to oncolytic viral therapy was evaluated by using HMGB1-blocking antibodies *in vitro* and in mice bearing intracranial tumors. IVIS and MRI imaging was utilized to visualize in real time virus spread, tumor growth, and changes in edema in mice. Our data showed that HMGB1 released in tumor microenvironment orchestrated increased vascular leakiness and edema. Further HMGB1 blocking antibodies rescued vascular leakiness and enhanced survival of intracranial glioma-bearing mice treated with oHSV.

INTRODUCTION

Oncolytic virus (OV) therapy utilizes cancer-cell specific replication-competent viruses to selectively kill cancer cells.¹ The recent US Food and Drug Administration (FDA) approval of Imlygic, an oncolytic herpes simplex virus (oHSV), for melanoma underscores the significance of this therapeutic modality.² Several other viruses are currently being evaluated for safety and efficacy in patients diagnosed with glioma and/or other solid tumors.³ While virus replication and ensuing tumor cell destruction is a prerequisite for oncolytic efficacy, activation of an anti-tumor immune response upon infection is also thought to contribute to efficacy.^{4,5} Strategies to maximize oHSV-mediated lytic effects while also harnessing host anti-tumor immunity are predicted to improve outcome for patients.⁶ Thus, a better understanding of changes induced in the tumor stroma by oHSV is essential to exploit maximal benefit.^{6,7}

HMGB1 is a ubiquitously expressed intracellular protein that binds DNA and transcription factors and regulates chromosomal structure and function.⁸ Under certain conditions, cells will release it into the extracellular environment, where it functions as damage-associated molecular pattern (DAMP). While most DAMPs are passively released by dying cells as a consequence of loss of membrane integrity, HMGB1 can also be actively released by cells upon stress via a poorly understood non-classical secretory pathway.⁹ In the extracellular environment, it orchestrates pro-inflammatory cytokine release and inflammation.^{9,10} Increased levels of secreted HMGB1 can be detected in serum of mice with sepsis and also in serum of septic patients suffering from an infection with a pathogen. Blockade of HMGB1 has been shown to increase survival of mice with lethal sepsis, and administration of HMGB1 proved lethal, implying that extracellular HMGB1 was a key player in mediating toxicity due to sepsis.¹¹ Released HMGB1 can exist in reduced or oxidized forms, depending on the redox state on the extracellular environment. In its reduced form, it partners with CXCL12 as a heterodimer to bind to and activate CXCR4 to stimulate tissue regeneration.¹² In its partially oxidized forms, it can bind to and activate signaling through TLR4 and RAGE receptor pathways. The complete oxidation of HMGB1 renders it inactive for both chemotactic and pro-inflammatory functions.¹³

Extracellular HMGB1 released upon asbestos-induced death of mesothelioma cells heralds the recruitment of tissue-healing macrophages, driving human malignant mesothelioma (MM) development and progression. Supporting this hypothesis, it has also been noted that HMGB1 blockade inhibits tumor growth

Received 31 October 2018; accepted 27 November 2018;
<https://doi.org/10.1016/j.omto.2018.11.005>.

Correspondence: Balveen Kaur, PhD, Department of Neurosurgery, McGovern Medical School, University of Texas Health Science Center, 6431 Fannin St., MSE R164, Houston, TX 77030, USA.

E-mail: balveen.kaur@uth.tmc.edu



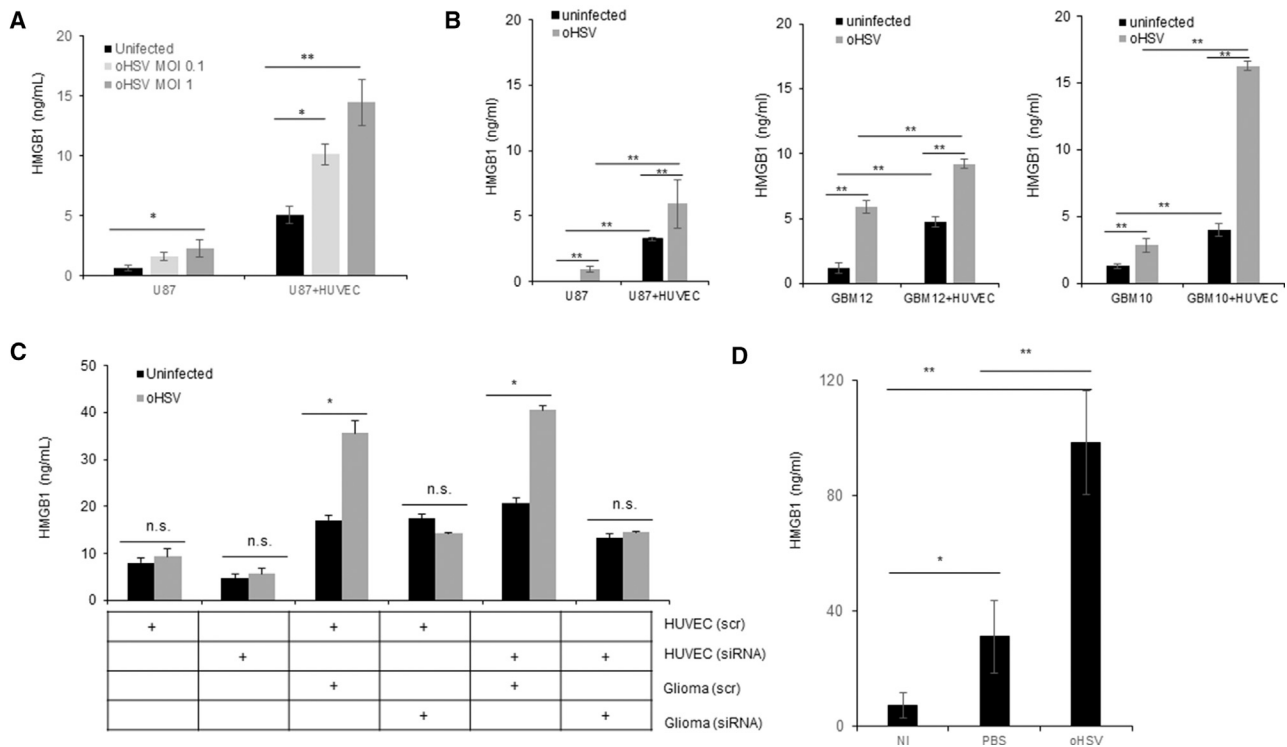


Figure 1. HMGB1 Is Released *In Vitro* and *In Vivo* during oHSV Tumor Therapy

(A) HMGB1 levels in conditioned medium from HSVQ-infected U87 glioblastoma cells (MOI = 0.1 or MOI = 1) and U87 cells infected with HSVQ and co-cultured with HUVEC cells (U87 + HUVEC). Conditioned medium was harvested 24 hr after treatment and HMGB1 levels measured by ELISA. Data shown are mean HMGB1 levels measured by ELISA in the conditioned medium \pm SD. (B) HMGB1 released in culture medium of the indicated cells after infection with HSVQ with or without HUVEC cell overlay as indicated (MOI = 0.1). HMGB1 secretion in the cells co-cultured with HUVEC was analyzed by ELISA. Data shown are mean HMGB1 levels measured by ELISA in the conditioned medium \pm SD. (C) HUVEC or U251 cells were transfected with either scrambled control or HMGB1 targeting siRNA. Control or HMGB1 siRNA-transfected glioma cells were infected with HSVQ (MOI = 0.01), and then the cells were overlaid with endothelial cells transfected with either scrambled control or HMGB1-targeting siRNA. 24 hr after treatment with HSVQ or no virus and HMGB1, levels were measured by ELISA. Data shown are mean HMGB1 levels measured by ELISA in the conditioned medium \pm SD. (D) Mice bearing intracranial GBM tumors were treated with HSVQ intratumorally (5×10^5 pfu/mouse). Five days later, serum was harvested and HMGB1 levels were measured by ELISA ($n = 5$ /group; NI, non-injected; PBS, saline-injected; oHSV, HSVQ-injected animals). * $p < 0.05$; ** $p < 0.01$.

in vitro, and prolonged survival of malignant mesothelioma-bearing mice *in vivo*.^{14,15} The extracellular release of HMGB1 has been noted upon infection with some oncolytic viruses (OVs), but its impact on the tumor microenvironment and/or virotherapy is not known. Here, we examined the release of HMGB1 in mice bearing tumors after oHSV treatment. Our results demonstrate that HMGB1 is secreted in serum of mice after oHSV therapy. This secretion depended on a cross-talk between tumor and stroma and HMGB1 neutralization in conjunction with oHSV improved survival of intracranial glioblastoma-bearing mice. *In vivo* imaging system (IVIS) and MRI imaging to visualize real-time tumor growth in mice revealed that HMGB1 blockade did not impact the growth rate of tumors with or without oHSV therapy but reduced tumor edema, contributing toward increased mice survival. Overall, our results demonstrate that blockade of HMGB1 can improve outcome in *in vivo* models after oHSV treatment and warrant further evaluation in its changes in patients as a prognostic marker for inflammation.

RESULTS

Glioblastoma Cells Actively Increase HMGB1 Secretion after oHSV Treatment

While HMGB1 release has been observed upon infection of murine fibroblasts,¹⁶ no significant release was noted upon HSV-1 infection of human and mouse breast cancer cells after infection with HSV-1 *in vitro*.^{17,18} To evaluate if HMGB1 is released after virotherapy of brain tumors, we infected primary patient derived GBM neurospheres and glioma cell lines and measured HMGB1 level released in the conditioned medium by ELISA after infection (Figures 1A and 1B). While there was a modest and dose-dependent increase in HMGB1 released by tumor cells upon infection with oHSV (Figure 1A) *in vitro*, this level was significantly higher when infected glioma cells were cultured with normal human endothelium cells (HUVECs) (Figures 1A and 1B). To understand the contribution of HUVEC cells to the released HMGB1 in the co-cultures, we repeated this co-culture in conditions where either glioma or endothelium cells were knocked down for HMGB1 using small interfering RNA

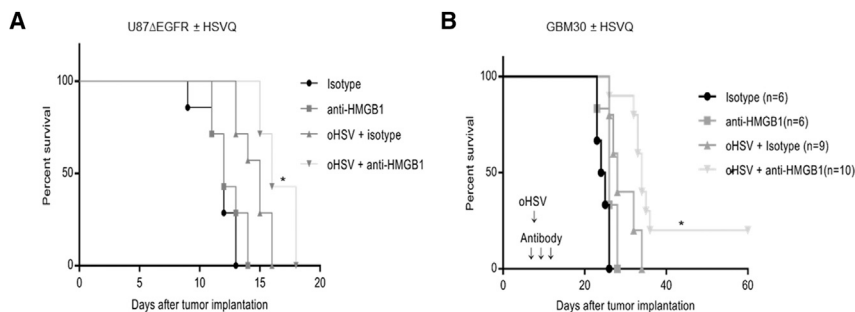


Figure 2. HMGB1 Blockade Prolongs oHSV-Treated GBM-Bearing Mice Survival

Kaplan-Meier survival curves of mice bearing intracranial U87ΔEGFR (A) ($n = 6/\text{group}$) or GBM30 (B) (and $n = 10/\text{group}$ for virus-treated animals with and without HMGB1 blockade and $n = 6/\text{group}$ for saline-treated animals with or without HMGB1-blocking antibodies) tumors treated with HMGB1 antibody or isotype control antibody (intraperitoneal on days 7, 8, and 9 post-tumor-implant). On day 8 after tumor implant, mice were randomized and injected with oHSV or saline (A, 5×10^5 pfu HSVQ for U87ΔEGFR; B, 1×10^5 pfu HSVQ for GBM30) by direct intratumoral injection. Mice

were euthanized when they showed signs of weight loss, hemiplegia, and paralysis or were found moribund as in accordance with our animal welfare care protocol. * $p < 0.05$ for anti-HMGB1 versus oHSV + anti-HMGB1 and oHSV + isotype versus oHSV + anti-HMGB1.

(siRNA). Quantification of HMGB1 released in conditioned medium revealed that endothelial cells did not release a significant amount of HMGB1 upon infection. Consistent with results shown above culture of HUVEC with infected glioma cells increased HMGB1 secretion. Knockdown of HMGB1 in endothelial cells did not affect the HMGB1 release in the co-culture, but knockdown of HMGB1 in glioma cells completely rescued HMGB1 release when infected glioma cells are cultured with HUVEC cells (Figure 1C). Together, this suggests a cross-talk between infected glioma and normal endothelial cells that contributed to increased HMGB1 secretion in the tumor microenvironment. To determine the *in vivo* relevance of HMGB1 released upon oHSV treatment, we treated mice bearing intracranial gliomas with PBS or oHSV (HSVQ, 5×10^5 plaque-forming units [pfu]/mouse) via direct intratumoral injection. Five days after virus injection, we collected serum from mice and assayed HMGB1 levels by ELISA. Figure 1D shows a significant increase in serum HMGB1 level in mice treated with oHSV, compared to PBS and no injection (NI) controls. The physical disruption of tissue is known to lead to HMGB1 release, which could be a consequence of active release or due to cell lysis (passive release). Since oHSV is delivered intratumorally by injections, it is important to discriminate the effect of active viral infection from physical disruption. Our results show that while saline injections do result in some released HMGB1, which can be measured in serum of mice, treatment of tumor-bearing mice with oHSV resulted in a 3.1-fold increase in HMGB1 over saline-injected tumors.

HMGB1 Blockade Prolongs Survival of GBM-Bearing Mice Treated with oHSV

To evaluate the *in vivo* significance of extracellular HMGB1 on oHSV therapeutic efficacy, we compared the survival of mice with established orthotopic glioblastoma tumors treated with oHSV in the presence and absence of HMGB1-blocking antibody. In brief, mice with orthotopic U87ΔEGFR glioma cells (Figure 2A) or patient-derived primary GBM (GBM30) cells (Figure 2B), were treated with isotype or HMGB1-blocking antibody on days 7, 8, and 9 after tumor implant. On day 8 post-tumor-implant, mice receiving isotype or HMGB1-blocking antibody were randomized and treated with a single dose of oHSV (5×10^5 pfu of HSVQ [Figure 2A] or 1×10^5 pfu HSVQ [Figure 2B]) or saline by direct intratumoral injection. Kaplan-

Meier survival curves of mice revealed that combination treatment with oHSV and HMGB1-blocking antibody significantly improved survival of mice over single therapies (Figures 2A and 2B).

Impact of Released HMGB1 on Virus Propagation *In Vitro* and *In Vivo*

To measure the impact of extracellular released HMGB1 on virus spread *in vitro*, we infected primary GBM neurospheres (GBM12 and GBM1016) and U87ΔEGFR glioma cell line with HSVQ in the presence or absence of HMGB1-blocking antibody and monitored virus propagation by flow cytometry. Quantification of GFP-positive cells (indicative of infected cells) in the presence or absence of HMGB1 blockade did not appear to significantly affect virus spread *in vitro* (Figure 3A). To evaluate the effect of HMGB1 on virus spread *in vivo*, we treated intracranial tumor-bearing mice with a single intratumoral injection of an oHSV encoding for luciferase on day 8 post-tumor-implant. Mice were treated intraperitoneally with isotype or HMGB1 blocking antibody on days 7, 8, and 9 after tumor cell implant. Virus-encoded luciferase activity was measured as a surrogate for virus propagation *in vivo* by IVIS imaging at various time points after intratumoral treatment of mice. Figures 3C and 3D show relative viral luciferase activity in the brains of mice treated with isotype or HMGB1-blocking antibody over time. All isotype-treated mice (Figure 3C, left panel) revealed an initial increase in virus spread (luciferase activity) followed by a decline after days 3–5, after which most control mice were euthanized in accordance with our IACUC guideline. HMGB1-blocking antibody-treated mice survived longer and showed a second burst of virus-encoded luciferase activity after day 5 post-virus-treatment (Figure 3C, right panel). Consistent with the previous results, mice treated with luciferase-expressing virus and HMGB1-blocking antibody survived longer than mice treated with virus alone (Figure 3B). In the first week after virus injection (when control and HMGB1-blocking-antibody-treated mice were both alive and could be compared), IVIS imaging (for virus-encoded luciferase) revealed a trajectory of initial increase in virus luciferase that showed an initial amplification of signal in the first couple of days followed by a decrease in signal intensity over time up to about a week. After a week of treatment, mice not treated with HMGB1-blocking antibody started succumbing to tumor burden. Thus, we can compare virus spread only in the first week between

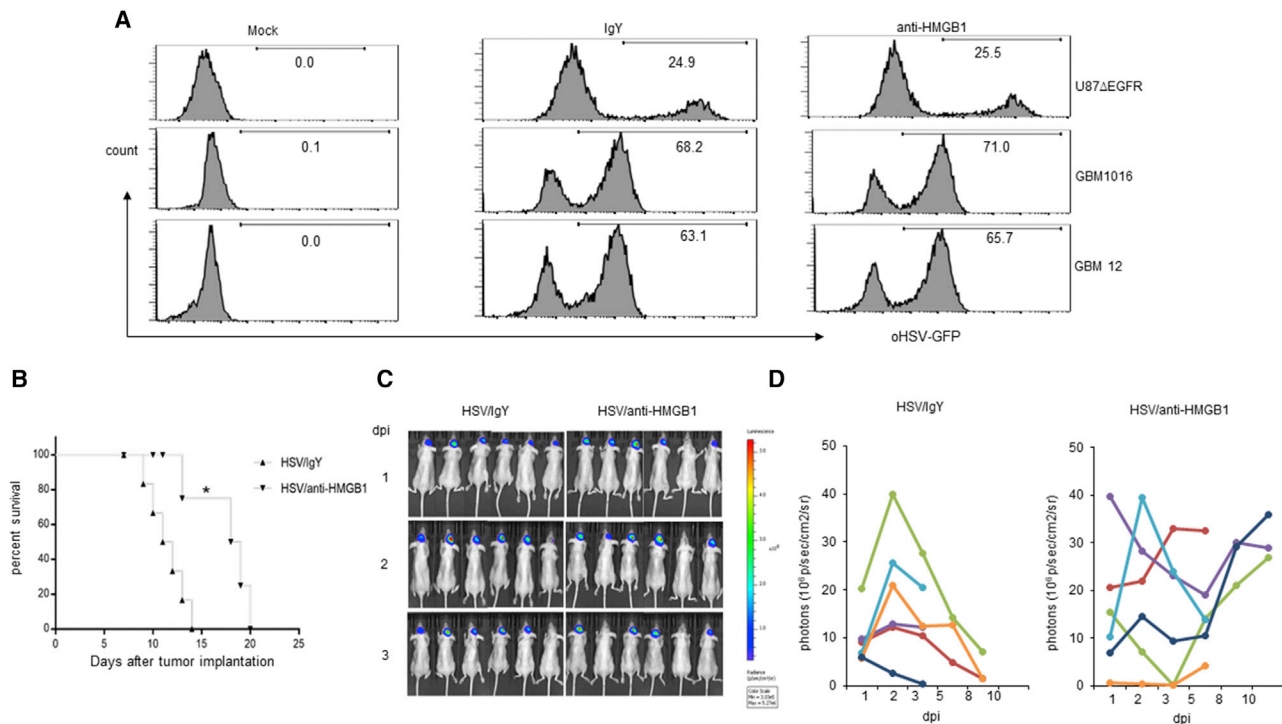


Figure 3. HMGB1 Blockade Does Not Affect oHSV Replication in GBM *In Vitro* and *In Vivo*

(A) GBM cell line (U87ΔEGFR) and patient-derived primary GBM cells (GBM12 and GBM1016) were infected with HSVQ (MOI = 0.5) for 1 hr and treated with anti-HMGB1 antibody or isotype IgY (10 μg/mL) for 48 hr. Percentage of GFP-positive virus-infected cells was analyzed by flow cytometry analysis. (B–D) Nude mice (n = 6/group) bearing intracranial U87ΔEGFR glioma cells were treated with 5×10^5 pfu of luciferase-expressing oHSV (HSVQ-Luc) by direct intratumoral injection 8 days post-tumor-implant. Mice were randomized to receive isotype or anti-HMGB1 (100 μg/mouse) blocking antibodies by i.p. injection for 3 days (–1, 0, 1 dpi of oHSV). (B) Kaplan-Meier survival curves of intracranial glioma-bearing mice treated with HSVQ-Luc with and without anti-HMGB1-blocking antibody treatment (*p < 0.05 for oHSV + anti-HMGB1 versus oHSV + IgY). n = 6/group. (C and D) Virus replication was monitored by IVIS imaging. (C) Representative images of mice showing virus-encoded luciferase activity over time. (D) Data shown are changes in relative luciferase activity in individual mice after treatment with HSVQ-Luc with isotype (left) or HMGB1-blocking antibody (right).

the two groups when the mice in the control group were still alive. In the first week after injection, IVIS imaging for virus-encoded luciferase revealed a trajectory of initial increase in virus luciferase that showed an initial amplification of signal in the first couple of days followed by a decrease in signal intensity over time up to about a week. We did not observe a statistically significant difference in luciferase signal intensity between isotype and HMGB1-blocking antibody-treated mice. Collectively, these results suggested that while HMGB1 blockade improved survival of mice, this could not be attributed to increased virus propagation *in vivo*.

Impact of HMGB1 on Intracranial Tumor Growth

HMGB1 has been described as both a cancer driver and suppressor,¹⁹ and so we evaluated the impact of HMGB1-blocking antibodies on intracranial glioma growth after virus therapy. In brief, mice bearing primary patient-derived GBM12-luciferase neurospheres or U87ΔEGFR luciferase (Figure 4A) expressing intracranial brain tumors were treated with oncolytic HSV (HSVQ) on day 15 (GBM12) or day 8 (U87ΔEGFR luciferase) post-tumor-implant. Mice were additionally treated with or without HMGB1-blocking antibodies 1 day before, the day of, and the day after oHSV treatment.

Tumor-cell-encoded-luciferase was imaged to visualize tumor growth over time. In both models, mice were sacrificed when they showed an overall body score of two or less or displayed clinical symptoms of paralysis, hemiparesis, or hemiplegia in accordance with our animal welfare protocol. IVIS imaging for tumor-encoded luciferase was monitored over time to evaluate the impact of HMGB1 blockade on tumor growth after virus therapy. Monitoring of tumor progression of individual mouse over time revealed that HMGB1 blockade did not affect the growth rate (comparing slopes of tumor growth) of tumors in both the tumor models (Figures 4B–4G). To compare changes in maximum tumor burden before euthanasia, we compared the mean of the maximal value of tumor-encoded luciferase recorded for each mouse treated with or without HMGB1-blocking antibody (Figures 4C and 4F) prior to euthanasia (dashed lines in Figures 4C and 4F). Mice treated with oHSVQ and HMGB1-blocking antibody appeared to display clinical symptoms meeting guidelines of euthanasia at a significantly larger tumor burden than mice treated with oHSV and isotype antibody control in both the models. These mice tolerated tumor better and survived longer and thus sustained a greater tumor burden at the time of euthanasia (Figures 4D and 4G). Collectively, these results indicate that while HMGB1 blockade

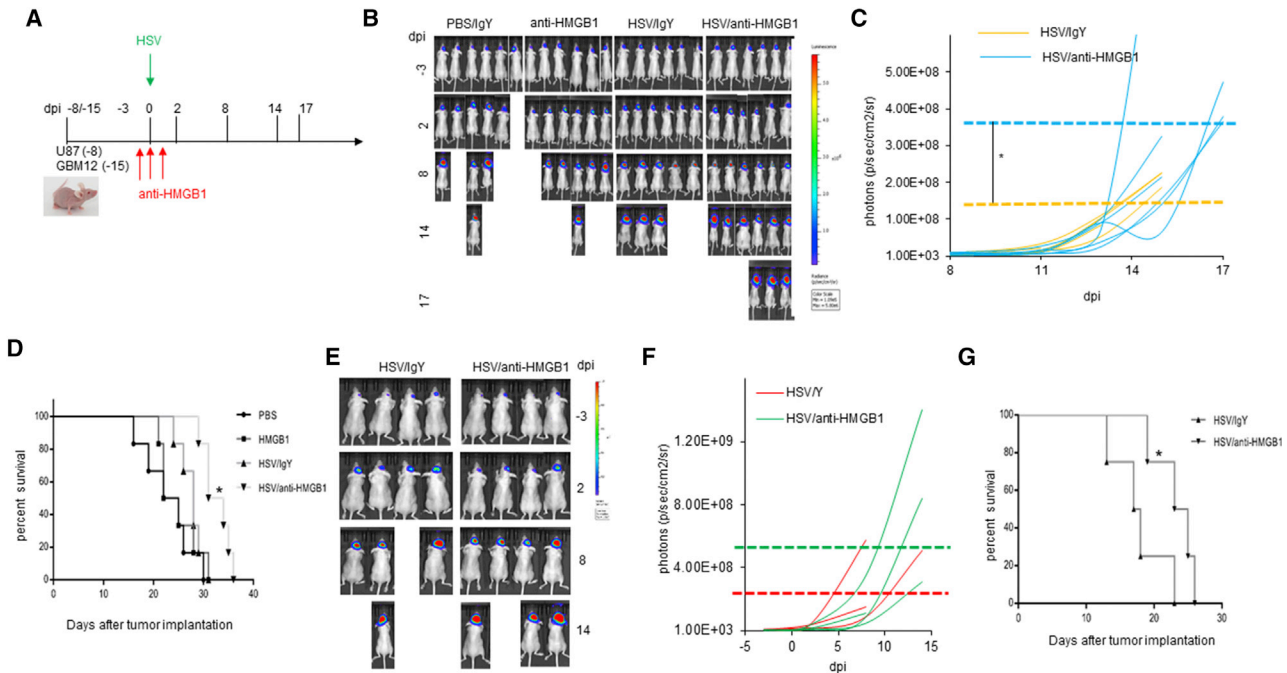


Figure 4. HMGB1 Blockade Does Not Inhibit Tumor Growth after oHSV Therapy

(A) Timeline of treatment schedule of mice implanted with either GBM12-luciferase or U87 Δ EFR luciferase-expressing glioma treated with oHSV with and without HMGB1-blocking antibody. (B) Representative images of mice bearing GBM12-luciferase cells showing tumor-encoded luciferase activity over time. (C) Data shown are relative luciferase activity of tumor-cell-expressed luciferase in individual mice treated with or without HMGB1-blocking antibodies in mice bearing GBM12-luciferase. The horizontal dashed lines indicate median values of maximal luciferase observed in mice from each group at the last measurable time point prior to death (n = 6/group). (D) Kaplan-Meier survival curves of mice shown in (B) and (C) (n = 6/group and *p < 0.05 between HSV/antiHMGB1 and HSV/IgY). (E) Representative images of mice bearing U87 Δ EGFR-luciferase cells showing tumor-encoded luciferase activity over time. Tumor growth in individual mice was measured by IVIS imaging. (F) Data shown are relative luciferase activity of tumor-cell-expressed luciferase in individual mice treated with or without HMGB1-blocking antibodies in mice bearing GBM12-Luc (C) (n = 6/group). The horizontal dashed lines indicate median values of maximal luciferase observed in mice from each group at the last measurable time point prior to death. (G) Kaplan-Meier survival curves of mice in (E) and (F).

during virus treatment kept symptoms of intracranial tumor burden controlled and kept mice alive longer, it did not affect tumor growth after virotherapy.

HMGB1-Induced Endothelial Activation in Tumor Microenvironment

Increased cerebral edema can lead to brain herniation, which is among the major factors resulting in GBM mortality.²⁰ Extracellular HMGB1 is known to have pro-inflammatory effects on endothelial cells manifested by increased vessel permeability and leukocyte adhesion mediated by increased expression of ICAM, VCAM, and RAGE.²¹ Hence, we investigated the impact of HMGB1 released by infected glioma cells on endothelial cell permeability. In brief, changes in endothelial cell permeability were evaluated by quantifying the passage of Evans blue conjugated to albumin into the bottom chamber of transwell chamber, lined by a confluent layer of HUVEC cells treated with conditioned medium from glioma cells treated with or without HSVQ virus in the presence or absence of HMGB1-blocking antibody. A significant increase in endothelial permeability was observed when endothelial cells were stimulated with conditioned medium

from oHSV-infected glioma cells. The addition of HMGB1-blocking antibodies rescued this leakiness, indicating that virus infection-mediated HMGB1 release could induce endothelial cell permeability (Figure 5A). Increased peripheral blood mononuclear cell (PBMC) adhesion to endothelial cells is also reflective of their activation. To measure the changes in endothelial-leukocyte interactions, fluorescence-labeled PBMCs were incubated with endothelial cells pre-treated with infected cell-conditioned medium with or without HMGB1-blocking antibodies. PBMCs were allowed to adhere to endothelial cells for 1 hr, at which point un-adhered PBMCs were washed off and total fluorescence attached to endothelial cells was quantified. Treatment of endothelial cells with infected-cell-conditioned medium increased PBMC adhesion to endothelium that was rescued in the presence of HMGB1-blocking antibodies (Figure 5B). Consistent with the increased adhesion, flow cytometry of endothelial cells cultured with oHSV-infected glioma cells revealed an induction of ICAM1 that was reduced in the presence of HMGB1-blocking antibodies (Figure 5C). To evaluate if this was reflective of an inhibition in viral infection by HMGB1 blockade in these co-cultures, we cultured cell-tracker orange-labeled endothelial cells with glioma cells

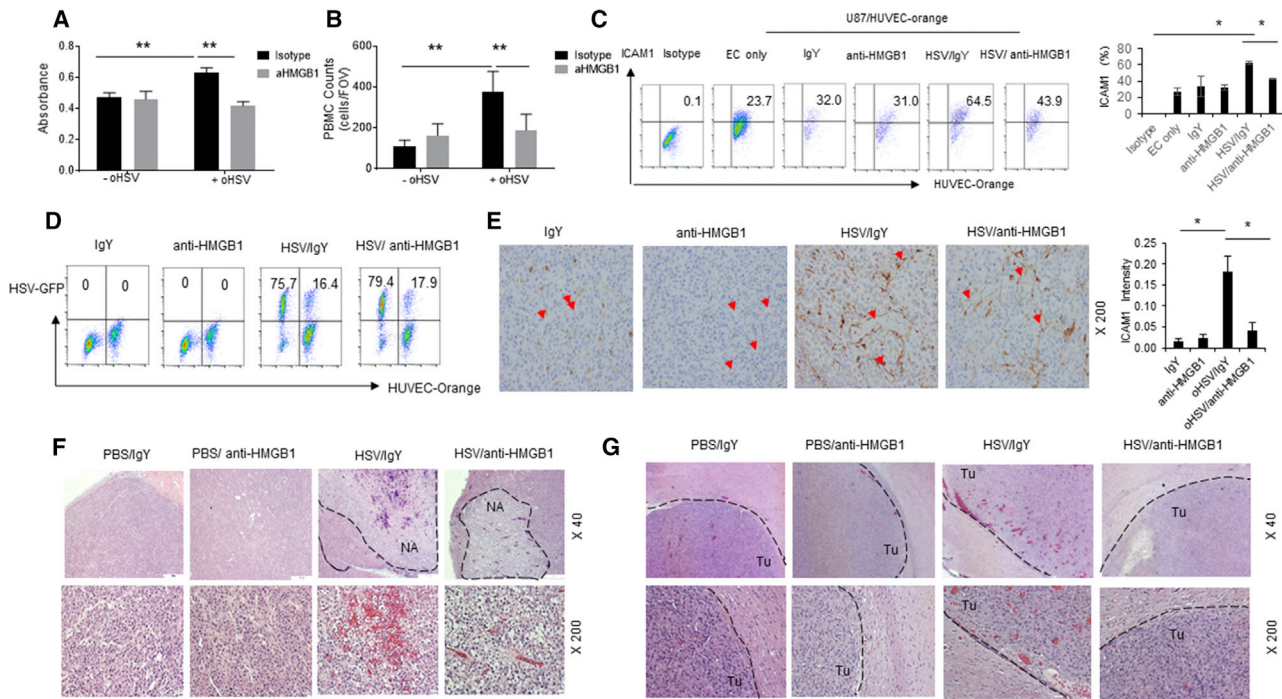


Figure 5. HMGB1 Blockade Inhibits Endothelial Cell Activation after oHSV treatment *In Vitro* and *In Vivo*

(A) Impact of HSVQ-released HMGB1 on vascular permeability was measured by the ability of Evans blue albumin to permeate through a monolayer of primary HUVEC cells. Monolayer of confluent HUVECs was seeded in the upper chamber of a boyden chamber, and the cells were treated with conditioned medium from infected glioma cell in the presence or absence of HMGB1-blocking antibody. Data shown are mean spectrophotometric quantitation of Evans blue dye that permeated through the monolayer. (B) Fluorescently labeled human donor PBMCs were incubated with HUVEC monolayer treated with conditioned medium from infected glioma cells in the presence or absence of HMGB1-blocking antibodies for 1 hr, and then unbound PBMCs were washed away. The number of PBMCs adhered to endothelial cells was quantified by measuring fluorescence. Data shown are mean fluorescence \pm SD. (C and D) HSVQ-infected U87 Δ EGFR cells were co-cultured with endothelial cells labeled with cell-tracker orange (HUVEC-orange) for 24 hr. U87 Δ EGFR cells were infected with or without oHSV for 1 hr and overlaid with HUVEC-orange cells treated with isotype control or HMGB1-blocking antibody. After 24 hr co-culture, cells were stained with ICAM1 antibody and the effect of HMGB1 neutralization on ICAM1 expression and oHSV replication is analyzed by flow cytometry. Representative dot plots for ICAM1 expression from one of three independent experiments is shown. Mean of three independent experiments \pm SD is shown on the right. (D) Dot blots of GFP-positive-infected cells with or without HMGB1 blockade. (E) Photomicrographs and quantification of intensity of IHC staining of ICAM1 expression in U87 Δ EGFR xenografts in nude mice. In brief, mice with subcutaneous U87 Δ EGFR xenografts were treated with HSVQ (1×10^5 pfu) or PBS when tumors reached 150–200 mm³. Mice were also treated with or without HMGB1-blocking antibody, 1 day after virus treatment. Two days post-virus-treatment, mice were euthanized, and harvested tumor sections were stained for ICAM1 (red arrowheads). Quantification of ICAM1 intensity was analyzed by ImageJ software (* $p < 0.05$ for oHSV + anti-HMGB1 versus oHSV + IgY, IgY, anti-HMGB1) ($n = 3$ mice/group and 10 images/section). (F and G) Photomicrographs of H&E staining of subcutaneous U87 Δ EGFR xenograft tumor (F) or intracranial GBM12 xenograft tumor sections (G). Mice with tumors were treated with an intratumoral injection of 5×10^5 pfu HSVQ/PBS with or without HMGB1 blockade as described above. Black dashed lines indicated tumor necrosis area (NA) after oHSV injection apparent in subcutaneous tumors. Black dashed line in (G) marks the interface between tumor (Tu) and normal brain tissue.

and measured percentage of GFP-positive infected cells in both glioma (orange negative) and endothelial cells (orange positive). Quantification of the percentage of infected cells revealed that the addition of HMGB1-blocking antibodies did not affect the rate of infection of glioma or endothelial cells when co-cultured (Figure 5D). To evaluate the effect of HMGB1-blocking antibody treatment on oHSV therapy-induced ICAM1 expression *in vivo*, tumor sections from mice bearing U87 xenografts treated with HSVQ in the presence or absence of HMGB1-blocking antibody were stained with ICAM1 antibody. Tumor sections from PBS-treated mice showed blood vessels that faintly stained for ICAM1. Consistent with the flow cytometry results, IHC staining of tumor sections from mice treated with HSVQ revealed virus-induced intense ICAM1 staining on tumor

vasculature, and that was rescued when virus-treated mice were also given HMGB1-blocking antibody (Figure 5E). Consistent with the increased endothelial cell activation, H&E staining of sections from subcutaneously implanted U87 Δ EGFR tumor (Figure 5F) and intracranial patient-derived primary GBM12 tumors (Figure 5G) revealed extensive erythrocyte extravasation in oHSV-treated tumors. This was significantly rescued in tumors treated with HMGB1-blocking antibodies in both subcutaneous and intracranial tumors.

HMGB1 Blockade Results in Reduced Edema *In Vivo*

Endothelial activation in traumatic CNS injuries has been known to result in edema. Thus, we evaluated changes in cerebral edema in intracranial glioma-bearing mice treated with oHSV in the presence

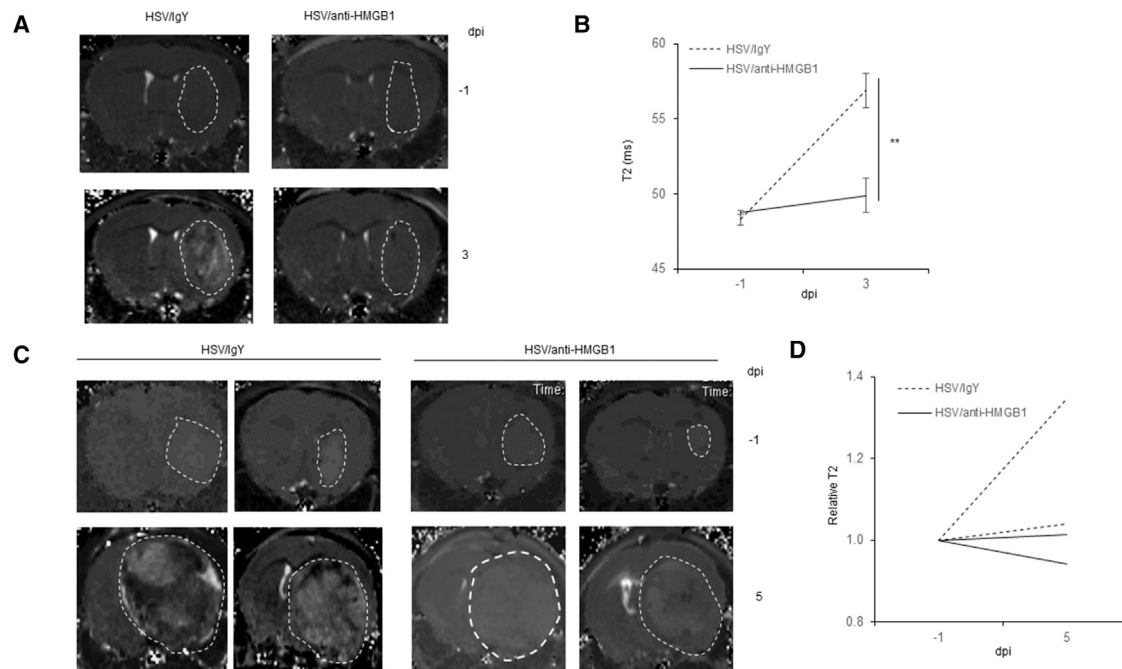


Figure 6. HMGB1 Blockade Reduces Brain Tumor Edema in GBM12 and U87ΔEGFR Model

Mice bearing intracranial GBM12-Luc (A) or U87ΔEGFR-Luc (B) tumor cells were inoculated into 5-week-old nude mice. 15 days (GBM12-Luc) or 8 days (U87ΔEGFR-Luc) later when tumors are visible under IVIS imaging, 5×10^5 pfu of HSVQ was injected into tumor-bearing mice by intra-tumoral injection. 100 μg of anti-HMGB1 neutralization antibody or isotype IgY was injected by intraperitoneal (i.p.) injection for 3 days (–1, 0, 1 dpi of virus). (A) Representative MRI-T2-weighted imaging (T2WI) images of a mouse bearing intracranial patient-derived primary GBM12 tumors ($n = 3$ /group). (B) Quantification of T2-weighted intensity in the tumor area of intracranial GBM12-bearing mice 1 day before and 3 days after virus treatment with or without HMGB1-blocking antibody. Data shown are mean intensity \pm SD. (C) Representative MRI-T2-weighted imaging (T2WI) images of mice bearing intracranial U87ΔEGFR tumors ($n = 2$ /group). (D) Quantification of relative change in T2-weighted intensity in individual mice 1 day before and 5 days after virus treatment with or without HMGB1-blocking antibody.

and absence of HMGB1 blockade.^{22,23} In brief, mice bearing intracranial GBM12 (Figures 6A and 6B) or U87 ΔEGFR tumors (Figures 6C and 6D) were treated with HSVQ (5×10^5 pfu) as described in the methods. Starting 1 day before virus injection mice were given daily intraperitoneal (i.p.) injections of HMGB1 blocking or isotype control antibody treatment for 3 days. Mice were also imaged using MRI-T2-weighted imaging (T2WI) to measure tumor-associated edema or water content 1 day prior to and 3 or 5 days after virotherapy. Images in Figure 6A and 6C are representative images of brains of tumor bearing mice 1 day before (top) and 3 or 5 days after (bottom) virotherapy with or without HMGB1-blocking antibody. White dashed lines outline the tumor area, and the increase in brightness of the T2WI signal after virotherapy is indicative of increased edema after virus treatment. Figure 6B represents quantification of T2WI signal in intracranial GBM12-bearing mice before and after virus therapy with isotype (dashed lines) or HMGB1-blocking antibody treatment ($n = 3$ /group). Virus treatment induced an increase in T2WI signal intensity that was rescued in mice treated with HMGB1-blocking antibody. Collectively, these findings indicate that oHSV therapy induces HMGB1 release in the tumor microenvironment, wherein the released HMGB1 heralds endothelial cell activation, which augments vascular leakiness and increases tissue edema.

DISCUSSION

HMGB1 is a DNA-binding nuclear protein that is highly expressed in many cancers. Its expression is associated with increased progression and angiogenesis of glioma.^{24,25} Extracellular HMGB1 can be passively released by dead or dying cells but is also actively released under some conditions.²⁶ For example, under interferon (IFN)γ stimulation, the activation and phosphorylation of Stat1 dimers results in the recruitment of histone acetylases, which result in the acetylation of HMGB1's nuclear localization signal.²⁷ This sequesters HMGB1 in the cytoplasm and results in its extracellular secretion. Once released extracellularly, HMGB1 can function as an alarmin by binding to and activating TLR and RAGE receptors on cell surface.^{28,29} Here, we have uncovered the release of HMGB1 *in vitro* and *in vivo* in glioma xenografts after virotherapy.

Extracellular HMGB1 (in its reduced form) has been shown to induce the production of CXCL12 and to also heterodimerize with it to activate CXCR4, thereby synergistically inducing CXCR4-driven tumor angiogenesis, growth, and invasion.^{30,31} It also mediates the recruitment of alternatively activated tumor-supportive macrophages, resulting in tumor growth and progression.³² Our results here revealed that HMGB1 blockade did not have a significant impact on tumor

growth or regression after oHSV therapy but did increase the survival of oHSV-treated mice. Paradoxically, while extracellular HMGB1 is well documented to be associated with tumor growth and promotion,³³ it can also augment the immunogenicity of cancer cells.³⁴ Blockade of HMGB1 with glycyrrhizin rescued the immunotherapeutic benefit of delivery of cytotoxic gene therapy to rats bearing intracranial tumors. Interestingly, treatment with glycyrrhizin did not rescue the subsequent tumor cell rejection of mice who had shown prior complete responses, indicating that while HMGB1 was important for the development of anti-tumor immunity, it did not play a role in elimination of glioma cells by established memory T cells. Future studies in immune-intact animal models will be essential to uncover the impact of HMGB1 on anti-tumor immunity after virotherapy.

Glycyrrhizin has been shown to bind to and inactivate extracellular HMGB1.²² Interestingly, it has also been shown to have a direct and potent anti-herpetic effect on cultured cells *in vitro* and has been associated with increased survival of mice with encephalitis.^{35–37} Contrary to the well-documented anti-viral effects of glycyrrhizin, a more recent study showed that direct incubation of mouse fibroblasts with glycyrrhizin led to a small increase in infected GFP-positive cells, with modest effects on oHSV-mediated cell toxicity, suggesting that there might be HMGB1-independent effects of glycyrrhizin on mouse fibroblast cultures.¹⁶ Here, we utilized HMGB1-blocking antibodies to understand the impact of HMGB1 on the tumor micro-environment after virotherapy. Our results here uncover that blockade of HMGB1 with a blocking antibody did not affect tumor growth and/or virus replication or spread in glioma cells *in vitro* and *in vivo*, but the observed survival advantage in glioma-bearing mice treated with oHSV and HMGB1-blocking antibody could be attributed to suppression of intracranial edema.^{21,32} This is corroborated by *in vitro* and *in vivo* observations of reduced endothelial activation and reduced edema in mice treated with HMGB1 blockade. Fully reduced HMGB1 increases the production of CXCL12 and also forms heterodimers with it to synergistically activate CXCR4, resulting in increased production of cell migration, vascular extravasation, and contribution to inflammation and edema.^{31,38} HMGB1 blockade after spinal cord injury has also been shown to suppress spinal cord edema and improve locomotor function in rats.²² Our data also uncovered that while mice injected with oHSV had an extended survival after HMGB1 blockade, HMGB1 blockade of PBS-treated mice did not augment survival. This can reflect the increased HMGB1 secretion observed after virotherapy compared to PBS-treated mice (Figure 1D) or changes in redox state of HMGB1 released³⁹ after virotherapy versus wound-healing response after injection alone. While we clearly see higher levels of HMGB1 released in serum of mice after virus treatment compared to PBS-treated mice, future studies will examine the effect of dose response and changes in the redox state of HMGB1 released after oHSV treatment. Since intracranial edema in GBM patients is well documented to result in brain swelling and clinical deterioration resulting in life-threatening complications.^{40,41} Our results suggest that monitoring HMGB1 levels in patients under-

going virotherapy could possibly be used to monitor intracranial inflammation and potentially life-threatening edema in patients with CNS tumors.

MATERIALS AND METHODS

Cell Lines, Reagents, Antibodies, and Viruses

U87- Δ EGFR human glioma cells and primary GBM neurospheres were cultured as described.⁴² HSVQ generation has been previously described.⁴³ Human umbilical vein endothelial cells (HUVEC, ATCC, Manassas, VA) were cultured in extracellular matrix (ECM) with supplements (ScienCell, Carlsbad, CA). HMGB1 was measured by ELISA kit (IBL International, Toronto, ON, Canada). All samples obtained from mouse were confirmed free of hemolysis as indicated by color. HMGB1-blocking or isotype control chicken immunoglobulin Y (IgY) antibodies were obtained from IBL International (Toronto, ON, Canada)

Co-culture Human GBM Cells with HUVEC

U87- Δ EGFR human glioma cells or the indicated primary GBM neurospheres were infected with the indicated virus for 1 hr. Uninfected virus was thoroughly washed off, and then the infected cells were overlaid with primary HUVEC cells for 24 hr. Culture supernatants were collected for ELISA of HMGB1. In some cases, the HUVEC cells were stained with cell tracker-orange (Thermo Scientific, Waltham, MA) per manufacturer's instructions. GFP-positive-infected and orange-positive endothelial cells were identified by flow cytometry analysis.

Flow Cytometry

The indicated cells were washed with PBS and stained with fluorescence-labeled primary antibody (ICAM1, BD Bioscience, San Jose, CA) in PBS containing 1% fetal bovine serum (FBS) for 30 min, followed by a PBS wash before analysis on a FACS Galios (Beckman Coulter, Brea, CA) flow cytometer. Data was analyzed by FlowJo software (FlowJo, Ashland, OR).

HMGB1 ELISA Assays

To quantify HMGB1 released from oHSV-infected cells, culture supernatants from indicated cells were collected and centrifuged at low speed to clear cell debris. HMGB1 concentration was measured by using an ELISA kit (IBL International, Toronto, ON, Canada) per manufacturer's guidelines.

Animal Surgery

All animal experiments were handled in accordance with the Subcommittee on Research Animal Care guidelines of the University of Texas Health Science Center at Houston and Ohio State University and have been approved by the Center for Laboratory Animal Medicine and Care (CLAMC). For intracranial mouse xenograft studies, female athymic nude mice were implanted intracranially with the indicated glioma cells, and the mice were treated with the indicated virus by a direct intra-tumor injection 8 days (U87 Δ EGFR, GBM30) or 15 days (GBM12) after tumor cell inoculation. HMGB1 blocking or isotype control chicken IgY antibodies (IBL International,

Toronto, ON, Canada) (100 µg/mouse) were administered by intraperitoneal injection on days -1, 0, and 1 after virus inoculation. Mice were either sacrificed at the indicated time or followed for survival. For subcutaneous mouse xenograft study, nude mice with U87ΔEGFR subcutaneous tumors (150–200 mm³) were treated with either HSVQ (1 × 10⁵ pfu) or PBS by direct intra-tumor injection. One day after virus treatment mice were also treated with either HMGB1 blocking or isotype control antibody. Three days after virus treatment, the animals were sacrificed and tumor tissue harvested and formalin fixed. Tissue sections were stained using ICAM1 (LSBio, Seattle, WA) and H&E.

Endothelial Cell Assays

EC cell permeability was measured using transwell chambers with a confluent layer of endothelial cells in the upper chamber. Permeability was quantified by spectrophotometric measurement of the Evans blue-labeled albumin (EBA) across confluent HUVEC monolayer. Adhesion of normal human-donor PBMCs to HUVECs was conducted using CytoSelect leukocyte-endothelium adhesion assay kit (Cell Biolabs, San Diego, CA) per the manufacturer's instructions.

Immunohistochemistry Staining

Paraffin-embedded GBM xenograft tumor tissue was processed with antigen retrieval, using pH 9.0 antigen retrieval buffer. The slides were blocked with 3% H₂O₂ and serum from the species of the secondary antibody. Slides were incubated with the primary antibody at 4°C overnight. Slides were washed and then incubated with secondary antibody for 20 min at room temperature. After washing, slides were developed with 3,3'-diaminobenzidine (DAB), counterstained with hematoxylin, and mounted for microscopy analysis.

IVIS Imaging

GBM12-luciferase, U87ΔEGFR-luciferase tumor growth, and HSV-luciferase replication were monitored by assessing luciferase activity with an IVIS (PerkinElmer, Waltham, MA). 150 mg/kg luciferin (Promega, Madison, WI) was administered into mice via intraperitoneal injection. After 1 min, the luciferin photon flux value was collected eight times with an exposure time of 30 s of 2 min interval.

MRI-Based Measurement Brain Edema

All MRIs were acquired on a 7 Tesla MRI scanner (Bruker Biospin, Billerica, MA). Animals were anesthetized with a 30:70 mixture of O₂ and medical air plus 1.5% isoflurane and placed prone in a cradle. A volume coil with an inner diameter of 72 mm for transmit, and 1 cm receive surface coil (Bruker Biospin, Billerica, MA) positioned on the head of the animals were used to acquire the images. T2-weighted MRI images were generated from multiecho spin-echo images and used to assess tumor edema. Acquisition parameters were as follows: TE = 10.6 ms, 10 echoes, TR = 3,190 ms, 15 image slices, 0.5-mm slice thickness, 150-mm in-plane resolution, Number of averages (NA) = 2. Software Paravision 5.1 (Bruker Biospin, Billerica, MA) was used to acquire the images and to calculate T2 relaxation time.

Statistical Analysis

All quantitative results are displayed as the mean ± SD. Statistical significance was determined using Prism5 software (GraphPad Software, La Jolla, CA). Kaplan-Meier analysis were used to estimate the survival over time, and log-rank test was performed to test the statistical significance. A p value less than 0.05 was considered to be statistically significant.

AUTHOR CONTRIBUTIONS

Conceptualization, B.K., B.H.; Methodology and Investigation, B.H., K.M., C.B., L.R., T.J.L., Y.B.-S., J.Y.Y., Y.Y., L.Y.B., K.H.B.; Writing, Review, and Editing, B.K., J.Y.Y.; Funding Acquisition and Supervision, B.K.

CONFLICTS OF INTEREST

The authors declare no competing interests.

ACKNOWLEDGMENTS

This study was funded by NINDS grant R01NS064607 and NCI grants R01CA150153 and P01CA163205 to B.K. and the Pelotonia research fellowship to L.R.

REFERENCES

- Lemay, C.G., Keller, B.A., Edge, R.E., Abei, M., and Bell, J.C. (2018). Oncolytic Viruses: The Best is Yet to Come. *Curr. Cancer Drug Targets* 18, 109–123.
- Kaufman, H.L., and Bines, S.D. (2010). OPTIM trial: a Phase III trial of an oncolytic herpes virus encoding GM-CSF for unresectable stage III or IV melanoma. *Future Oncol.* 6, 941–949.
- Russell, L., and Peng, K.W. (2018). The emerging role of oncolytic virus therapy against cancer. *Linchuan Zhongliuxue Zazhi* 7, 16.
- Bommarreddy, P.K., Shettigar, M., and Kaufman, H.L. (2018). Integrating oncolytic viruses in combination cancer immunotherapy. *Nat. Rev. Immunol.* 18, 498–513.
- Alvarez-Breckenridge, C., Kaur, B., and Chiocca, E.A. (2009). Pharmacologic and chemical adjuvants in tumor virotherapy. *Chem. Rev.* 109, 3125–3140.
- Wojton, J., and Kaur, B. (2010). Impact of tumor microenvironment on oncolytic viral therapy. *Cytokine Growth Factor Rev.* 21, 127–134.
- Haseley, A., Boone, S., Wojton, J., Yu, L., Yoo, J.Y., Yu, J., Kurozumi, K., Glorioso, J.C., Caligiuri, M.A., and Kaur, B. (2012). Extracellular matrix protein CCN1 limits oncolytic efficacy in glioma. *Cancer Res.* 72, 1353–1362.
- Di, X., He, G., Chen, H., Zhu, C., Qin, Q., Yan, J., Zhang, X., and Sun, X. (2018). High-mobility group box 1 protein modulated proliferation and radioresistance in esophageal squamous cell carcinoma. *J. Gastroenterol. Hepatol.* Published online July 3, 2018. <https://doi.org/10.1111/jgh.14371>.
- Bianchi, M.E., Crippa, M.P., Manfredi, A.A., Mezzapelle, R., Rovere Querini, P., and Venereau, E. (2017). High-mobility group box 1 protein orchestrates responses to tissue damage via inflammation, innate and adaptive immunity, and tissue repair. *Immunol. Rev.* 280, 74–82.
- Rovere-Querini, P., Capobianco, A., Scaffidi, P., Valentini, B., Catalanotti, F., Giazoni, M., Dumitriu, I.E., Müller, S., Iannaccone, M., Traversari, C., et al. (2004). HMGB1 is an endogenous immune adjuvant released by necrotic cells. *EMBO Rep.* 5, 825–830.
- Wang, H., Bloom, O., Zhang, M., Vishnubhakat, J.M., Ombrellino, M., Che, J., Frazier, A., Yang, H., Ivanova, S., Borovikova, L., et al. (1999). HMG-1 as a late mediator of endotoxin lethality in mice. *Science* 285, 248–251.
- Lee, G., Espirito Santo, A.I., Zwingerberger, S., Cai, L., Vogl, T., Feldmann, M., Horwood, N.J., Chan, J.K., and Nanchahal, J. (2018). Fully reduced HMGB1 accelerates the regeneration of multiple tissues by transitioning stem cells to G_{Alert}. *Proc. Natl. Acad. Sci. USA* 115, E4463–E4472.

13. Palmblad, K., Schierbeck, H., Sundberg, E., Horne, A.C., Harris, H.E., Henter, J.I., Antoine, D.J., and Andersson, U. (2015). High systemic levels of the cytokine-inducing HMGB1 isoform secreted in severe macrophage activation syndrome. *Mol. Med.* *20*, 538–547.
14. Jube, S., Rivera, Z.S., Bianchi, M.E., Powers, A., Wang, E., Pagano, I., Pass, H.I., Gaudino, G., Carbone, M., and Yang, H. (2012). Cancer cell secretion of the DAMP protein HMGB1 supports progression in malignant mesothelioma. *Cancer Res.* *72*, 3290–3301.
15. Pellegrini, L., Xue, J., Larson, D., Pastorino, S., Jube, S., Forest, K.H., Saad-Jube, Z.S., Napolitano, A., Pagano, I., Negi, V.S., et al. (2017). HMGB1 targeting by ethyl pyruvate suppresses malignant phenotype of human mesothelioma. *Oncotarget* *8*, 22649–22661.
16. Sprague, L., Lee, J.M., Hutzen, B.J., Wang, P.Y., Chen, C.Y., Conner, J., Braidwood, L., Cassady, K.A., and Cripe, T.P. (2018). High Mobility Group Box 1 Influences HSV1716 Spread and Acts as an Adjuvant to Chemotherapy. *Viruses* *10*, E132.
17. Takasu, A., Masui, A., Hamada, M., Imai, T., Iwai, S., and Yura, Y. (2016). Immunogenic cell death by oncolytic herpes simplex virus type 1 in squamous cell carcinoma cells. *Cancer Gene Ther.* *23*, 107–113.
18. Workenhe, S.T., Simmons, G., Pol, J.G., Lichty, B.D., Halford, W.P., and Mossman, K.L. (2014). Immunogenic HSV-mediated oncolysis shapes the antitumor immune response and contributes to therapeutic efficacy. *Mol. Ther.* *22*, 123–131.
19. Seidu, R.A., Wu, M., Su, Z., and Xu, H. (2017). Paradoxical Role of High Mobility Group Box 1 in Glioma: A Suppressor or a Promoter? *Oncol. Rev.* *11*, 325.
20. Silbergeld, D.L., Rostomily, R.C., and Alvord, E.C., Jr. (1991). The cause of death in patients with glioblastoma is multifactorial: clinical factors and autopsy findings in 117 cases of supratentorial glioblastoma in adults. *J. Neurooncol.* *10*, 179–185.
21. Fiuza, C., Bustin, M., Talwar, S., Tropea, M., Gerstenberger, E., Shelhamer, J.H., and Suffredini, A.F. (2003). Inflammation-promoting activity of HMGB1 on human microvascular endothelial cells. *Blood* *101*, 2652–2660.
22. Sun, L., Li, M., Ma, X., Zhang, L., Song, J., Lv, C., and He, Y. (2018). Inhibiting high mobility group box-1 reduces early spinal cord edema and attenuates astrocyte activation and aquaporin-4 expression after spinal cord injury in rats. *J. Neurotrauma*. Published online October 4, 2018. <https://doi.org/10.1089/neu.2018.5642>.
23. Yang, L., Wang, F., Yang, L., Yuan, Y., Chen, Y., Zhang, G., and Fan, Z. (2018). HMGB1 a-Box Reverses Brain Edema and Deterioration of Neurological Function in a Traumatic Brain Injury Mouse Model. *Cell. Physiol. Biochem.* *46*, 2532–2542.
24. Yang, Y., Huang, J.Q., Zhang, X., and Shen, L.F. (2015). MiR-129-2 functions as a tumor suppressor in glioma cells by targeting HMGB1 and is down-regulated by DNA methylation. *Mol. Cell. Biochem.* *404*, 229–239.
25. Bassi, R., Giussani, P., Anelli, V., Colleoni, T., Pedrazzi, M., Patrone, M., Viani, P., Sparatore, B., Melloni, E., and Riboni, L. (2008). HMGB1 as an autocrine stimulus in human T98G glioblastoma cells: role in cell growth and migration. *J. Neurooncol.* *87*, 23–33.
26. Kang, R., Zhang, Q., Zeh, H.J., 3rd, Lotze, M.T., and Tang, D. (2013). HMGB1 in cancer: good, bad, or both? *Clin. Cancer Res.* *19*, 4046–4057.
27. Lu, B., Antoine, D.J., Kwan, K., Lundbäck, P., Wähämaa, H., Schierbeck, H., Robinson, M., Van Zoelen, M.A., Yang, H., Li, J., et al. (2014). JAK/STAT1 signaling promotes HMGB1 hyperacetylation and nuclear translocation. *Proc. Natl. Acad. Sci. USA* *111*, 3068–3073.
28. Gardella, S., Andrei, C., Ferrera, D., Lotti, L.V., Torrisi, M.R., Bianchi, M.E., and Rubartelli, A. (2002). The nuclear protein HMGB1 is secreted by monocytes via a non-classical, vesicle-mediated secretory pathway. *EMBO Rep.* *3*, 995–1001.
29. Bonaldi, T., Talamo, F., Scaffidi, P., Ferrera, D., Porto, A., Bachi, A., Rubartelli, A., Agresti, A., and Bianchi, M.E. (2003). Monocytic cells hyperacetylate chromatin protein HMGB1 to redirect it towards secretion. *EMBO J.* *22*, 5551–5560.
30. Abu El-Asrar, A.M., Mohammad, G., Nawaz, M.I., and Siddiquei, M.M. (2015). High-Mobility Group Box-1 Modulates the Expression of Inflammatory and Angiogenic Signaling Pathways in Diabetic Retina. *Curr. Eye Res.* *40*, 1141–1152.
31. Schiraldi, M., Raucci, A., Muñoz, L.M., Livoti, E., Celona, B., Venereau, E., Apuzzo, T., De Marchis, F., Pedotti, M., Bachi, A., et al. (2012). HMGB1 promotes recruitment of inflammatory cells to damaged tissues by forming a complex with CXCL12 and signaling via CXCR4. *J. Exp. Med.* *209*, 551–563.
32. Yang, H., Pellegrini, L., Napolitano, A., Giorgi, C., Jube, S., Preti, A., Jennings, C.J., De Marchis, F., Flores, E.G., Larson, D., et al. (2015). Aspirin delays mesothelioma growth by inhibiting HMGB1-mediated tumor progression. *Cell Death Dis.* *6*, e1786.
33. He, S., Cheng, J., Sun, L., Wang, Y., Wang, C., Liu, X., Zhang, Z., Zhao, M., Luo, Y., Tian, L., et al. (2018). HMGB1 released by irradiated tumor cells promotes living tumor cell proliferation via paracrine effect. *Cell Death Dis.* *9*, 648.
34. Candolfi, M., Yazig, K., Foulad, D., Alzadeh, G.E., Tesarfreund, M., Muhammad, A.K., Puntel, M., Kroeger, K.M., Liu, C., Lee, S., et al. (2009). Release of HMGB1 in response to proapoptotic glioma killing strategies: efficacy and neurotoxicity. *Clin. Cancer Res.* *15*, 4401–4414.
35. Sekizawa, T., Yanagi, K., and Itoyama, Y. (2001). Glycyrrhizin increases survival of mice with herpes simplex encephalitis. *Acta Virol.* *45*, 51–54.
36. Sabouri Ghannad, M., Mohammadi, A., Safiallah, S., Faradmal, J., Azizi, M., and Ahmadvand, Z. (2014). The Effect of Aqueous Extract of Glycyrrhiza glabra on Herpes Simplex Virus 1. *Jundishapur J. Microbiol.* *7*, e11616.
37. Pompei, R., Flore, O., Marccialis, M.A., Pani, A., and Loddo, B. (1979). Glycyrrhizic acid inhibits virus growth and inactivates virus particles. *Nature* *281*, 689–690.
38. Yun, J., Jiang, G., Wang, Y., Xiao, T., Zhao, Y., Sun, D., Kaplan, H.J., and Shao, H. (2017). The HMGB1-CXCL12 Complex Promotes Inflammatory Cell Infiltration in Uveitogenic T Cell-Induced Chronic Experimental Autoimmune Uveitis. *Front. Immunol.* *8*, 142.
39. Lorenzen, I., Mullen, L., Bekeschus, S., and Hanschmann, E.M. (2017). Redox Regulation of Inflammatory Processes Is Enzymatically Controlled. *Oxid. Med. Cell. Longev.* *2017*, 8459402.
40. Palombi, L., Marchetti, P., Salvati, M., Osti, M.F., Frati, L., and Frati, A. (2018). Interventions to Reduce Neurological Symptoms in Patients with GBM Receiving Radiotherapy: From Theory to Clinical Practice. *Anticancer Res.* *38*, 2423–2427.
41. Chae, S.S., Kamoun, W.S., Farrar, C.T., Kirkpatrick, N.D., Niemeyer, E., de Graaf, A.M., Sorensen, A.G., Munn, L.L., Jain, R.K., and Fukumura, D. (2010). Angiopoietin-2 interferes with anti-VEGFR2-induced vessel normalization and survival benefit in mice bearing gliomas. *Clin. Cancer Res.* *16*, 3618–3627.
42. Yoo, J.Y., Hurwitz, B.S., Bolyard, C., Yu, J.G., Zhang, J., Selvendiran, K., Rath, K.S., He, S., Bailey, Z., Eaves, D., et al. (2014). Bortezomib-induced unfolded protein response increases oncolytic HSV-1 replication resulting in synergistic antitumor effects. *Clin. Cancer Res.* *20*, 3787–3798.
43. Hardcastle, J., Kurozumi, K., Dmitrieva, N., Sayers, M.P., Ahmad, S., Waterman, P., Weissleder, R., Chiocca, E.A., and Kaur, B. (2010). Enhanced antitumor efficacy of vasculostatin (Vstat120) expressing oncolytic HSV-1. *Mol. Ther.* *18*, 285–294.